

# Stretch-Induced Crystallization through Single Molecular Force Generating Mechanism

Yuanhua Cong,<sup>†</sup> Hao Liu,<sup>‡</sup> Daoliang Wang,<sup>†</sup> Baijin Zhao,<sup>†</sup> Tingzi Yan,<sup>†</sup> and Liangbin Li<sup>\*,†,‡</sup>

<sup>†</sup>National Synchrotron Radiation Lab and College of Nuclear Science and Technology, University of Science and Technology of China, Hefei, China

<sup>‡</sup>CAS Key Lab for Softmatter Chemistry, University of Science and Technology of China, Hefei, China

Wei Chen and Zhiyuan Zhong

Biomedical Polymers Laboratory, Key Laboratory of Organic Synthesis of Jiangsu Province, College of Chemistry, Chemical Engineering and Materials Science, Soochow University, Suzhou, China

Ming-Champ Lin and Hsin-Lung Chen

Department of Chemical Engineering, National Tsing Hua University, Hsin-Chu, Taiwan

Chuanlu Yang

Department of Physics and Electrons, Ludong University, Yantai, China

## INTRODUCTION

Flow-induced crystallization is a long-standing nonequilibrium thermodynamic challenge in physics, which is of importance in material science as well as in food and biological systems. Processing of polymer generally undergoes a flow-induced crystallization process, which results in diverse structures and controls the final properties. Though a great effort has been dedicated in this field for more than half a century, no satisfactory molecular theory is established yet.<sup>1,2</sup> Theoretically, a simple thermodynamic approach is to incorporate the external work with Gibbs free energy, which substantially reduces the nucleation barrier and thus enhances the nucleation rate.<sup>3</sup> Experimentally, however, it is far more difficult to evenly distribute macroscopic external work to individual molecule, which prevents most theoretical models from being quantitatively tested by experiments.<sup>4</sup>

Imposing a flow on polymer melt leads to a significant increase of nucleation rate and may result in shish-kebab structure, which heterogeneously distributes in space. The polydispersity of chain length may be partly responsible for the heterogeneity, though the roles of short and long chains on flow-induced nucleation are still under debate.<sup>5–8</sup> More evidently, the instabilities of polymer flow such as melt fracture, shear banding, and wall slip deviate the local field from the apparent macroscopic flow completely.<sup>9</sup> Without information about flow at molecular level, any efforts to connect apparent shear rate and relaxation time of molecular chain through Weissenberg or Deborah number may take the risk of making unacceptable deviations. The ideal approach is to impose an external work on an individual molecule directly. This has been achieved through single molecular force spectroscopy with atomic force microscopy, optic tweezers, etc., and revealed rich structural transitions at individual chain level.<sup>10</sup>

Unfortunately, those methodologies cannot be borrowed to study phase transitions in a condensed state system with numerous chains. Therefore, an innovative approach is crucial to solve flow-induced crystallization in the condensed system.

In this work, we employ a double crystallizable symmetry diblock copolymer poly(L-lactide)-*b*-poly(ethylene oxide) (PLLA-*b*-PEO) to solve this challenge, where we let PLLA block to stretch PEO block as they are covalently linked with each other. Because of their rich phase behavior, block copolymers have been widely employed as a model system to study crystallization.<sup>11–42</sup> A schematic illustration of our idea is presented in Figure 1. As the melting temperature of PLLA is about 100 °C higher than that of PEO, it is possible to crystallize PLLA in a wide temperature window where PEO remains in melt. Increasing the crystallization temperature  $T_{C-PLLA}$  of PLLA leads to an increase of lamellar thickness  $l_{PLLA}$  of PLLA as  $l_{PLLA}$  is inversely proportional to supercooling  $\Delta T$ . Correspondingly, the thickness  $l_{PEO}$  of PEO layer also proportionally increases as the volume ratio between the two blocks is nearly constant. Varying crystallization temperature of PLLA, different strains can be imposed on PEO block. As each PEO chain is connected with an individual PLLA block through covalent bond, every PEO chain sustains the same strain and stress statistically. A similar idea was already employed to study crowding transition of polymer brush by Chen et al.<sup>43–45</sup> Our idea is also inspired from microphase separation of block copolymer in strong segregation limit, where stretch of chain is balanced by the surface free energy.<sup>46</sup> Compared to microphase separation, crystallization of

Received: June 2, 2011

Revised: July 5, 2011

Published: July 14, 2011

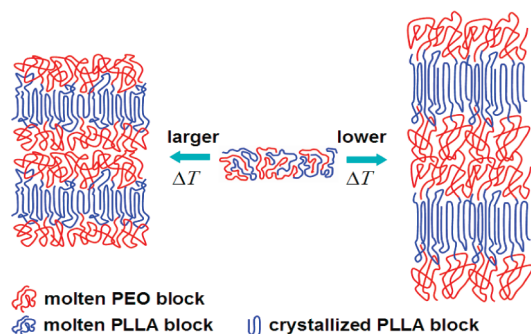


**Figure 1.** Schematic illustration of PLLA-*b*-PEO single molecular force generating mechanism.

one block can generate larger strains, which is also tunable through controlling the crystallization temperature. Following this approach, the idea of single molecular force generating mechanism is achieved in the condensed system and allows us to study stretch-induced crystallization of polymer at the single molecular level.

## EXPERIMENTAL SECTION

**Materials.** The symmetric diblock copolymer PLLA-*b*-PEO used in this work has number-average molecular weights of both blocks of 5000 g/mol and a distribution of 1.05, which was synthesized through a ring-open polymerization.<sup>47</sup>

**Characterization.** In situ small-angle X-ray scattering (SAXS) measurements were performed using a Bruker Nanostar SAXS instrument equipped with a two-dimensional position-sensitive detector (Bruker AXS) with  $512 \times 512$  channels. The radiation wavelength  $\lambda$  is 0.1541 nm. SAXS with synchrotron radiation source is also employed to study the layer structure, which is performed at BL16B1 of Shanghai Synchrotron Radiation Facility (SSRF) and BL23A1 of National Synchrotron Radiation Research Center (NSRRC) ( $\lambda = 0.1541$  nm).

Differential scanning calorimetry (DSC) experiments were measured on a TA Instruments 2000 DSC which was calibrated using an indium standard with a precision of  $\pm 0.2$  °C. The samples were encapsulated in hermetically sealed aluminum pans.

**Experimental Procedure.** For isothermal crystallization, the sample was kept in a brass sample holder with Kapton windows as a sandwich structure. It was first heated up to 170 °C and kept for 5 min on a hot stage (an accessory of Nanostar, with a precision of  $\pm 0.1$  °C). Subsequently, it was cooled to the crystallization temperature of PLLA block ( $T_{C-PLLA}$ , 90, 100, 110, 120, and 130 °C). Note no microphase separation occurs before crystallization of PLLA blocks. Thus, crystallization of PLLA starts from a homogeneous phase, which results into periodic layer structure with PLLA and PEO nanodomains arranged alternatively. When crystallization of PLLA block was finished, the system was quickly cooled to 45.5 °C for isothermal crystallization of PEO block. The whole procedure was in vacuum to prevent possible degradation at high temperatures. SAXS measurements were taken during isothermal crystallization with 10 min per frame.

The nonisothermal experiments of PEO block were carried out by DSC. All samples were treated as follows. First, specimens underwent an isothermal processing at the crystallization temperature of PLLA as above. After completion of crystallization of PLLA block, they were quickly transferred to DSC for the fixed

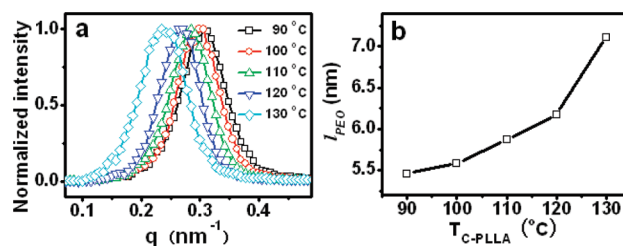


**Figure 2.** (a) Five SAXS curves for PLLA-*b*-PEO copolymer first undergoes isothermal crystallization at different  $T_{C-PLLA}$  (all of them were promptly collected when they are cooled to 45.5 °C). (b) Plot of  $l_{PEO}$  vs crystallization temperature of PLLA.

cooling rate experiment. And then the sample was cooled to  $-50$  °C at a rate of 10 °C/min for the recording of the crystallization exotherms in a nitrogen atmosphere.

## RESULTS AND DISCUSSION

Figure 2a plots the SAXS intensity curves of samples after PLLA block isothermally crystallized at different temperatures (PEO remains in melt). The  $x$ -axis  $q = 4\pi \sin \theta / \lambda$  is the modulus of scattering vector, where  $2\theta$  is the scattering angle and  $\lambda$  is the X-ray wavelength. With the increase of crystallization temperature, the scattering peak shifts to low  $q$  direction continuously. On the basis of the  $q$  value of SAXS peak in Figure 2a and Bragg law  $L = 2\pi/q$ , the long period  $L$  of PLLA-*b*-PEO is obtained. DSC measurements show that the crystallinity of PLLA is rather constant of about 60% at different  $T_{C-PLLA}$ , which indicates that some segments of PLLA blocks still remain in amorphous state. Based on SAXS curves, electron density profile of the layer structure is constructed,<sup>48–51</sup> which indicates that amorphous PLLA segments are mainly located at the interface between PLLA lamellar crystal and PEO melt. The existence of this interface amorphous PLLA layer is reasonable. As crystallization of PLLA block imposes stretching on its covalently linked PEO block, PLLA block is also suffered a counterforce. The compromise between enthalpy gain of PLLA and entropy loss of PEO blocks is expected to hinder the crystallization of PLLA, which may force part of PLLA segments remaining in amorphous state at the interface between PLLA lamellar crystal and PEO melt.

Taking the crystallinity of PLLA, the density of PEO melt ( $1.124$  g cm<sup>-3</sup>),<sup>52</sup> and the densities of crystalline and amorphous PLLA ( $1.290$  and  $1.248$  g cm<sup>-3</sup>),<sup>53</sup> the PEO layer thickness  $l_{PEO}$  is calculated and plotted vs  $T_{C-PLLA}$  in Figure 2b. As expected,  $l_{PEO}$  increases with  $T_{C-PLLA}$ . Note the layer spacing estimated through this approach is consistent with the result from electron density reconstruction. Through this approach, we realize imposing different strains and stresses on PEO blocks. The strength imposed on PEO blocks can be estimated with reduced tethering density of PEO blocks  $\tilde{\sigma}$ , which is defined as  $\tilde{\sigma} = \pi N_A l_{PEO} \rho_{M-PEO} R_g^2 / M_n$ .<sup>54</sup> Here  $N_A$ ,  $\rho_{M-PEO}$ ,  $M_n$ , and  $R_g$  are the Avogadro constant, the density of PEO melt,<sup>52</sup> number-average molecular weight, and radius of gyration of tethered PEO chain in an unperturbed conformation in melt, respectively.  $R_g$  was calculated according to  $\langle R_g^2 \rangle = Nb^2/6$ , where  $N$  and  $b$  are the number of Kuhn monomer and the Kuhn length, respectively.<sup>55</sup> The physical significance of  $\tilde{\sigma}$  is the number of the tethered chains in the area  $\pi R_g^2$  which is covered by an end free chain in the same condition.<sup>43–45,54</sup> The lowest  $\tilde{\sigma}$  calculated is 17.68 with a  $T_{C-PLLA}$  of 90 °C, which is already much larger than the critical

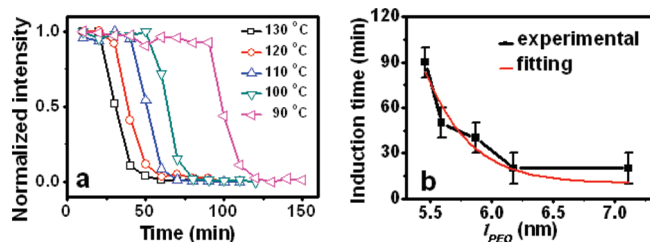


**Figure 3.** (a) Evolution of normalized  $I(q)$  during crystallization of PEO at 45.5 °C. The PLLA-*b*-PEO samples with the PLLA blocks initially isothermally crystallized at temperatures indicated in the Figure. (b) Plot of the induction time of PEO crystallization vs  $l_{PEO}$ .

value of the onset of highly stretched brush regime ( $>14.3$ ).<sup>44</sup> This indicates that all of the PEO chains in current work locate in the highly stretched regime where they suffer strongly stress.

With information on strain in hand, we proceed to study the stretch-induced isothermal crystallization of PEO block at 45.5 °C with in situ SAXS measurements. After crystallization of PEO block, the electron density  $\rho_{e-PEO}$  of PEO layer increases. As the scattering intensity  $I(q)$  is proportional to the square of the electron density contrast between two phases ( $\Delta\rho_e = \rho_{e-PLLA} - \rho_{e-PEO}$ , the electron density difference between PLLA and PEO layers), the crystallization of PEO blocks leads to a decrease of  $I(q)$ , which enable us to track the crystallization process of PEO. Figure 3a shows the time evolution of the normalized  $I(q)$  of samples with different initial  $T_{C-PLLA}$ , which corresponds to different strains on the PEO blocks. With higher  $T_{C-PLLA}$  (where the PLLA blocks imposed larger strain on the PEO blocks), the crystallization of the PEO blocks take place much earlier, which is consistent with the reports on flow-induced crystallization of polymer. As we mainly focus on stretch-induced nucleation process, the induction time of crystallization is extracted from Figure 3a, which represents nucleation rate. For the convenience of later discussion, we plot the induction time vs  $l_{PEO}$  instead of  $T_{C-PLLA}$  in Figure 3b, as  $l_{PEO}$  represents the strain and the reduced tethering density of PEO block directly. The induction time of PEO crystallization decreases monotonically with the increase of  $l_{PEO}$  or the strain. With the lowest strain ( $l_{PEO} \approx 5.46$  nm), the induction time is about 90 min, while increasing  $l_{PEO}$  to 7.11 nm leads a reduction of the induction time to 20 min. Intriguingly, the growth rate is almost independent of this spacing (deduced from the decay of the normalized intensity in Figure 3a). Highly stretching imposed on PEO blocks may hinder diffusion during crystal growth, which may compensate the enhancement on surface nucleation and leads to similar overall growth rate.

Single molecular stretch-induced nucleation of PEO is also demonstrated with DSC measurements in a nonisothermal crystallization process. Similar with SAXS experiments, the samples with isothermally crystallized PLLA blocks were cooled down to let PEO crystallize with a cooling rate of 10 °C/min. The heat flow traces during cooling are presented in Figure 4a. A clearly progressive shift of the single exothermic peak toward high temperature is observed with increase of  $T_{C-PLLA}$ . We take the onset temperatures of crystallization to indicate the nucleation rate of PEO, which are plotted vs  $l_{PEO}$  in Figure 4b. Bearing small strain with a  $l_{PEO}$  of 5.46 nm, PEO starts to crystallize at about 32.7 °C, whereas a large strain with a  $l_{PEO}$  of 7.11 nm leads the onset temperature to being 38.0 °C. The nonisothermal crystallization behavior further confirms the enhancement of

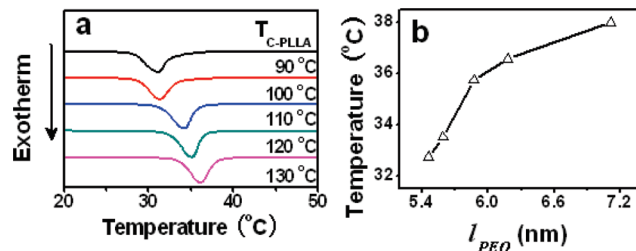


**Figure 4.** (a) A set of DSC curves of the PLLA-*b*-PEO samples during cooling scan. The samples with the PLLA blocks initially isothermally crystallized at temperatures indicated in the figure. (b) Plot of the onset temperature of crystallization vs  $l_{PEO}$ .

nucleation induced by single molecular stretching. Note domain volume may also affect nucleation rate.<sup>56</sup> Nevertheless, in our work a small variation of the spacing of PEO (from 5.46 to 7.11 nm) leads to a relatively large drop of  $T_{C-PEO}$  (from 32.7 to 38 °C), which cannot be accounted only considering size effect if we refer to the data in ref 56. According to classical nucleation theory, nucleation is only involving local density fluctuation. If a system is significantly larger than the primary nucleus, it should not affect nucleation. The volume effect may also be possibly related to surface tension.

How does the single molecular stretch generated by PLLA block enhance the nucleation rate of PEO? Stretching PEO chain generated by surface crowding leads to an increase of free energy of PEO melt, which correspondingly reduces nucleation barrier  $\Delta G^*$  and increases thermodynamic driving force  $\Delta G = G_L - G_S$  (the free energy difference between liquid phase  $G_L$  and crystal  $G_S$ ). Based on the nucleation theory proposed by Lauritzen and Hoffman, the rate of nucleation  $N_q$  with zero strain can be expressed as<sup>57,58</sup>

$$N_q = CkT_C\Delta G \exp\left(-\frac{E_a}{kT_C}\right) \exp\left[-\frac{K_n}{T_C(\Delta G)^n}\right] \quad (1)$$

where  $k$ ,  $C$ ,  $T_C$ , and  $E_a$  are the Boltzmann constant, a constant, crystallization temperature, and activation energy of diffusion, respectively.  $K_n$  is a constant containing energetic and geometrical factor of the nucleus. The exponent  $n$ , appearing also as a subscript for  $K$ , accounts for different kinds of nucleation. For primary nucleation, the exponent  $n = 2$  and  $K_2/T_C$  is given by  $32\sigma_e\sigma^2/(kT_C\rho_{C-PEO}^2)$ , where  $\sigma_e$  and  $\sigma$  are the end and the lateral surface free energy, respectively, and  $\rho_{C-PEO}$  is the density of PEO crystal (1.239 g cm<sup>-3</sup>).<sup>52</sup> Stretch contributes an extra work ( $\Delta G_f$ ) to increase thermodynamic driving force ( $\Delta G$ ). Assuming  $E_a$  is not affected by stretch, the ratio between  $N_q$  and the nucleation rate  $N_f$  under strain can be expressed as<sup>3</sup>

$$\frac{N_q}{N_f} = \frac{1}{1 + \Delta G_f/\Delta G_q} \exp\left[\frac{K_2}{T_C(\Delta G_q)^2} \left(\frac{1}{(1 + \Delta G_f/\Delta G_q)^2} - 1\right)\right] \quad (2)$$

The ratio of nucleation rates with different strains can be approximately represented by the inverse ratio of the induction time ( $t_{iq}$  at quiescent and  $t_{if}$  under stretching), namely

$$t_{if} = \frac{t_{iq}}{1 + \Delta G_f/\Delta G_q} \exp\left[\frac{K_2}{T_C(\Delta G_q)^2} \left(\frac{1}{(1 + \Delta G_f/\Delta G_q)^2} - 1\right)\right] \quad (3)$$

Following theory of polymer brush in highly stretched regime,<sup>59</sup> the free energy change due to stretching can be expressed as

$$\Delta G_f = \frac{\pi^2 k T_C N_A}{16 N M b^2} l_{PEO}^2 \quad (4)$$

where  $N$  is number of segments with Kuhn length of  $b$ ,  $M$  molecular weight of PEO block, and  $N_A$  the Avogadro number. Inserting eq 4 into eq 3, we can fit the data in Figure 3b with eq 3 to obtain  $K_2/T_C$  (the fitting curve is also shown in Figure 3b), which gives  $K_2/T_C = (1.80 \pm 0.58) \times 10^4 \text{ J}^2 \text{ g}^{-2}$  with a  $y$ -shift factor added in the equation. Note the existence of the shift factor is reasonable, which indicates an induction time is still required even when the chains are fully extended. The fitting result of  $y$ -shift factor is 10 min, lower than the minimum induction time (20 min), which is also acceptable. As the lateral surface free energy is not expected to vary with crystallization condition, we take  $\sigma = 10.6 \text{ erg cm}^{-2}$  from Cheng and Kovacs<sup>60,61</sup> to estimate the end surface free energy  $\sigma_e$  of stretch-induced nuclei. The calculated  $\sigma_e$  in our case is  $34.0 \pm 10.9 \text{ erg cm}^{-2}$ , which is comparable with the value for folded-chain surface reported by Cheng and Kovacs ( $22.4 \text{ erg cm}^{-2}$ ).<sup>60,61</sup> The good correlation suggests that combining classical nucleation theory with the extra work  $\Delta G_f$  in the driving force can be generalized to all flow-induced crystallization.

Compared to flow-induced crystallization with a macroscopic flow field, our single molecular force generating mechanism avoids the miscorrelation between the parameters of flow and molecular conformation due to uneven distribution of the work of flow field in both molecular and macroscopic scales. This miscorrelation sets intrinsic obstacle for the development of molecular theory of flow-induced crystallization, though macroscopic statistics on phenomenological correlation may be still valid. The single molecular force generating method demonstrated in this work is a quasi-thermodynamic process, which allows us to correlate molecular strain with nucleation quantitatively. This is an important step toward the final establishment of the molecular theory for flow-induced crystallization of polymer in the nonequilibrium thermodynamic circumstance, where polymer dynamics has to be introduced in.

## CONCLUSIONS

In summary, a symmetric diblock copolymer PLLA-*b*-PEO is devised to realize stretching single molecule in a condensed system. Because of the quasi-statically stretching by PLLA block, the nucleation rate of PEO crystal is accelerated. The free energy of the stretched single chain is incorporated with the classical nucleation theory, which accounts for the acceleration of nucleation rate quantitatively.

## AUTHOR INFORMATION

### Corresponding Author

\*E-mail: lbli@ustc.edu.cn.

## ACKNOWLEDGMENT

The authors thank Prof. Stephen Z. D. Cheng (Akron), Prof. Wim H. de Jeu (Umass), Prof. Bernard Lotz (Strasbourg), Prof. Jerold Schultz (Delaware), Prof. Goran Ungar (Sheffield), Prof. Zhengang Wang (Caltech), Prof. Wenbing Hu (Nanjing), and Prof. Yongfeng Men (Changchun) for valuable discussions. This

work is supported by the National Natural Science Foundation of China (51033004, 50973103, 20774091, 20904050), the Fund for One Hundred Talent Scientist of CAS, 973 program of MOST (2010CB934504), and the experimental fund of NSRL.

## REFERENCES

- (1) Miller, R. L. *Flow-induced Crystallization in Polymer Systems*; Gordon and Breach: New York, 1979.
- (2) Li, L. B.; De Jeu, W. H. *Adv. Polym. Sci.* **2005**, *181*, 75–120.
- (3) Coppola, S.; Grizzuti, N.; Maffettone, P. L. *Macromolecules* **2001**, *34*, 5030–5036.
- (4) Graham, R. S.; Olmsted, P. D. *Phys. Rev. Lett.* **2009**, *103*, 115702.
- (5) Kimata, S.; Sakurai, T.; Nozue, Y.; Kasahara, T.; Yamaguchi, N.; Karino, T.; Shibayama, M.; Kornfield, J. A. *Science* **2007**, *316*, 1014–1017.
- (6) Hsiao, B. S.; Yang, L.; Somani, R. H.; Avila-Orta, C. A.; Zhu, L. *Phys. Rev. Lett.* **2005**, *94*, 117802.
- (7) Zhao, B. J.; Li, X. Y.; Huang, Y. J.; Cong, Y. H.; Ma, Z.; Shao, C. G.; An, H. N.; Yan, T. Z.; Li, L. B. *Macromolecules* **2009**, *42*, 1428–1432.
- (8) Balzano, L.; Kukalyekar, N.; Rastogi, S.; Peters, G. W. M.; Chadwick, J. C. *Phys. Rev. Lett.* **2008**, *100*, 048302.
- (9) Tapadia, P.; Ravindranath, S.; Wang, S. Q. *Phys. Rev. Lett.* **2006**, *96*, 196001.
- (10) Neuman, K. C.; Nagy, A. *Nature Methods* **2008**, *5*, 491–505.
- (11) Reiter, G.; Castelein, G.; Sommer, J. U. *Phys. Rev. Lett.* **2001**, *87*, 226101.
- (12) Darko, C.; Botiz, I.; Reiter, G.; Breiby, D. W.; Andreasen, J. W.; Roth, S. V.; Smilgies, D. M.; Metwalli, E.; Papadakis, C. M. *Phys. Rev. E* **2009**, *79*, 041802.
- (13) Hong, S.; MacKnight, W. J.; Russell, T. P.; Gido, S. P. *Macromolecules* **2001**, *34*, 2398–2399.
- (14) Shin, D.; Shin, K.; Aamer, K. A.; Tew, G. N.; Russell, T. P. *Macromolecules* **2005**, *38*, 104–109.
- (15) Lutkenhaus, J. L.; McEnnis, K.; Serghei, A.; Russell, T. P. *Macromolecules* **2010**, *43*, 3844–3850.
- (16) Miranda, D. F.; Russell, T. P.; Watkins, J. J. *Macromolecules* **2010**, *43*, 10528–10535.
- (17) Wei, X. Y.; Li, L.; Kalish, J. P.; Chen, W.; Russell, T. P. *Macromolecules* **2011**, *44*, 4269–4275.
- (18) Li, L. B.; S  r  ro, Y.; Koch, M. H. J.; De Jeu, W. H. *Macromolecules* **2003**, *36*, 529–532.
- (19) Li, L. B.; Zhong, Z. Y.; De Jeu, W. H.; Dijkstra, P. J.; Feijen, J. *Macromolecules* **2004**, *37*, 8641–8646.
- (20) Li, L. B.; Lambrea, D.; de Jeu, W. H. *J. Macromol. Sci., Phys.* **2004**, *B43*, 59–70.
- (21) Li, L. B.; Meng, F. H.; Zhong, Z. Y.; Byelov, D.; De Jeu, W. H.; Feijen, J. *J. Chem. Phys.* **2007**, *126*, 024904.
- (22) Rottele, A.; Thurn-Albrecht, T.; Sommer, J. U.; Reiter, G. *Macromolecules* **2003**, *36*, 1257–1260.
- (23) Nandan, B.; Hsu, J. Y.; Chen, H. L. *J. Macromol. Sci., Polym. Rev.* **2006**, *46*, 143–172.
- (24) Loo, Y. L.; Register, R. A.; Ryan, A. J. *Phys. Rev. Lett.* **2000**, *84*, 4120.
- (25) Loo, Y. L.; Register, R. A.; Ryan, A. J. *Macromolecules* **2002**, *35*, 2365–2374.
- (26) Loo, Y. L.; Register, R. A. In *Developments in Block Copolymer Science and Technology*; Hamley, I. W., Ed.; John Wiley & Sons: New York, 2004; pp 213–243.
- (27) Hobbs, J. K.; Register, R. A. *Macromolecules* **2006**, *39*, 703–710.
- (28) Hamley, I. W.; Fairclough, P. J. A.; Ryan, A. J.; Bates, F. S.; Towns-Andrews, E. *Polymer* **1996**, *37*, 4425–4429.
- (29) Fairclough, P. J. A.; Mai, S. M.; Masten, M. W.; Bras, W.; Messe, L.; Turner, S. C.; Gleeson, A. J.; Booth, C.; Hamley, I. W.; Ryan, A. J. *J. Chem. Phys.* **2001**, *114*, 5425–5431.

- (30) Hamley, I. W.; Fairclough, P. J. A.; Terrill, N. J.; Ryan, A. J.; Lipic, P. M.; Bates, F. S.; Towns-Andrews, E. *Macromolecules* **1996**, *29*, 8835–8843.
- (31) Castillo, R. V.; Müller, A. J. *Prog. Polym. Sci.* **2009**, *34*, 516–560.
- (32) Müller, A. J.; Balsamo, V.; Arnal, M. L. *Adv. Polym. Sci.* **2005**, *190*, 1–63.
- (33) Müller, A. J.; Albuerno, J.; Marquez, L.; Raquez, J. M.; Degée, P.; Dubois, P.; Hobbs, J.; Hamley, I. W. *Faraday Discuss.* **2005**, *128*, 231–252.
- (34) Michell, R. M.; Müller, A. J.; Castelletto, V.; Hamley, I. W.; Deshayes, G.; Dubois, P. *Macromolecules* **2009**, *42*, 6671–6681.
- (35) Cai, C.; Wang, L.; Dong, C. M. *J. Polym. Sci., Part A: Polym. Chem.* **2006**, *44*, 2034–2044.
- (36) Wu, T.; He, Y.; Fan, Z. Y.; Wei, J.; Li, S. M. *Polym. Eng. Sci.* **2008**, *48*, 425–433.
- (37) Huang, C. I.; Tsai, S. H.; Chen, C. M. *J. Polym. Sci., Part B: Polym. Phys.* **2006**, *44*, 2438–2448.
- (38) Kim, K. S.; Chung, S.; Chin, I. J.; Kim, M. N.; Yoon, J. S. *J. Appl. Polym. Sci.* **1999**, *72*, 341–348.
- (39) Yang, J. L.; Zhao, T.; Zhou, Y. C.; Liu, L. J.; Li, G.; Zhou, E. L.; Chen, X. S. *Macromolecules* **2007**, *40*, 2791–2797.
- (40) Kubies, D.; Rypáček, F.; Kovářová, J.; Lednický, F. *Biomaterials* **2000**, *21*, 529–536.
- (41) Zhu, L.; Cheng, S. Z. D.; Calhoun, B. H.; Ge, Q.; Quirk, R. P.; Thomas, E. L.; Hsiao, B. S.; Yeh, F. J.; Lotz, B. *J. Am. Chem. Soc.* **2000**, *122*, 5957–5967.
- (42) Pfeifferkorn, D.; Kyremateng, S. O.; Busse, K.; Kammer, H. W.; Thurn-Albrecht, T.; Kressler, J. *Macromolecules* **2011**, *44*, 2953–2963.
- (43) Chen, W. Y.; Zheng, J. X.; Cheng, S. Z. D.; Li, C. Y.; Huang, P.; Zhu, L.; Xiong, H. M.; Ge, Q.; Guo, Y.; Quirk, R. P.; Lotz, B.; Deng, L. F.; Wu, C.; Thomas, E. L. *Phys. Rev. Lett.* **2004**, *93*, 028301.
- (44) Zheng, J. X.; Xiong, H. M.; Chen, W. Y.; Lee, K.; Van Horn, R. M.; Quirk, R. P.; Lotz, B.; Thomas, E. L.; Shi, A. C.; Cheng, S. Z. D. *Macromolecules* **2006**, *39*, 641–650.
- (45) Hsiao, M. S.; Zheng, J. X.; Van Horn, R. M.; Quirk, R. P.; Thomas, E. L.; Chen, H. L.; Lotz, B.; Cheng, S. Z. D. *Macromolecules* **2009**, *42*, 8343–8352.
- (46) Semenov, A. N. *Macromolecules* **1993**, *26*, 6617–6621.
- (47) Hiemastra, C.; Zhong, Z. Y.; Li, L. B.; Dijkstra, P. J.; Feijen, J. *Biomacromolecules* **2006**, *7*, 2790–2795.
- (48) Zeng, X. B.; Ungar, G. *Polymer* **1998**, *39*, 4523–4533.
- (49) Ungar, G.; Zeng, X. B.; Brooke, G. M.; Mahammed, S. *Macromolecules* **1998**, *31*, 1875–1879.
- (50) Zeng, X. B.; Ungar, G. *Macromolecules* **2001**, *34*, 6945–6954.
- (51) Zeng, X. B.; Ungar, G.; Spells, S. J.; Brooke, G. M.; Farren, C.; Harden, A. *Phys. Rev. Lett.* **2003**, *90*, 155508.
- (52) Wunderlich, B. *Macromolecular Physics, Crystal Structure, Morphology, Defects*; Academic: New York, 1973; Vol. 1.
- (53) Fischer, E. W.; Hans, J. S.; Wegner, G. *Kolloid Z. Z. Polym.* **1973**, *251*, 980–990.
- (54) Kent, M. S. *Macromol. Rapid Commun.* **2000**, *21*, 243–270.
- (55) Rubinstein, M.; Colby, R. H. *Polymer Physics*; Oxford University Press: New York, 2003.
- (56) Massa, V. M.; Carvalho, J. L.; Dalnoki-Veress, K. *Phys. Rev. Lett.* **2006**, *97*, 247802.
- (57) Lauritzen, J. I.; Hoffman, J. D. *J. Rev. Natl. Bur. Stand* **1960**, *64A*, 73–102.
- (58) Ziabicki, A. *Colloid Polym. Sci.* **1996**, *274*, 705–716.
- (59) Wang, Z. G.; Safran, S. A. *J. Chem. Phys.* **1991**, *94*, 679–687.
- (60) Cheng, S. Z. D.; Chen, J. H.; Janimak, J. J. *Polymer* **1990**, *31*, 1018–1024.
- (61) Kovacs, A. J.; Straupe, C.; Gonthier, A. J. *Polym. Sci., Polym. Symp.* **1977**, *59*, 31–54.